ASPECTS REGARDING THE STUDY OF HYDRAULIC AND MECHANICAL PARAMETERS OF A "SPIDER CRANE" SYSTEM

NICUŞOR BAROIU[1] [*], VIOREL PĂUNOIU[1], VIRGIL GABRIEL TEODOR[1], GEORGIANA-ALEXANDRA MOROŞANU[1], RĂZVAN SEBASTIAN CRĂCIUN[1]

[1] "Dunărea de Jos" University of Galati, Faculty of Engineering, 47 Domnească Street, Galati, 800008, Romania
Correspondence: Nicusor.Baroiu@ugal.ro

Abstract: Since it is acknowledged that transport and lifting installations play an extremely important role in industry, construction, and the extractive field, as well as in the mechanization of loading-unloading works, the movement of equipment or materials, special attention is paid to the growth and diversification of such installations at the level of the most advanced technologies. The paper presents the operating principles and characteristics of a lifting and transport installation known as a "Spider Crane". This installation is considered a more cost-effective and efficient alternative to traditional cranes for works where lifting requirements are below certain limits and significant heights. Thus, an analysis of the hydraulic lifting system is carried out, based on the calculation of hydraulic fluid flows for the drive pumps, the specific speeds and forces of the hydraulic cylinders, a mechanical analysis of the clamping system with hook, as well as a finite element analysis of some mechanical and hydraulic components.

Keywords: "Spider Crane", lifting system, hydraulic pump, hydraulic motor, hook, FEM

1. INTRODUCTION

As technologies advance and the increase in the level of industrialization requires a more comprehensive approach, the construction of new buildings, shopping centers etc. becomes more and more difficult to achieve due to the lack of space in areas that do not allow the handling of objects with an ordinary crane. This led to the creation of a new type of crane called "Spider Crane". The spider crane has a wide usage in various fields, especially in the narrow spaces where large-capacity cranes cannot enter. Due to its shape, it is able to fit through most doors, allowing access to areas previously inaccessible to standard cranes, Figure 1 [1-3].

" Spider Crane" lifting systems have been analyzed from several perspectives, emphasizing on investigating and performing static structural analysis based on lifting load, range [4, 5], hydraulic system analysis or analysis of some mechanical components of the complex lifting group.

Thus, T. Sevdim et al. [4] performed a study aimed at reducing vibrations at the end of the cranes arm through a structural static analysis, under different loading conditions, for a spider crane designed to lift a load of 0-500 kg, by using ANSYS software. Statistics reveal that the spider crane can lift 1200 kg before reaching the plastic region,

therefore its safety factor is 2.4 when lifting 500 kg, and its natural frequencies are 16.2 Hz and 50 Hz. A finite element analysis in ANSYS to validate the strength of a crane chassis structure is performed by Li et al. [5] based on the stress distribution, noting that the stress on the chassis structure is much lower than the allowable stress of the material. Similarly, A.A. Shaikh et al. [6], using a structural static analysis in ANSYS, reveals that the tipping load decreases with the increase in the load radius, defining the stability factor by calculating the overturning loads. Scenarios regarding the tandem use of two cranes with mobile counterweights of the same type were presented by S. Rishmawi [7], who performed a pseudodynamic stability analysis of overturning stability, studying the effect of acceleration controls, travel distances and other parameters of the crane if the payload to be lifted is oversized or irregular in shape.

Fig. 1. Spider cranes [1-3].

CAD elements with facilities provided by various graphic design environments and theoretical algorithms are frequently used for modeling moving or actuation and control elements [8-10]. A.K. Kamath et al. presents the modeling and control of a cabled "Spider Crane" mechanism, in which the cable and pulley dynamics are decoupled and the payload is viewed as a pendulum suspended from a cable whose suspension point is on a table moving in a two-dimensional space, performing various simulations in the MATLAB software program [11].

The hydraulic lifting system is considered one of the most important elements of the crane. The hydraulic system of spider cranes is divided into several components, the most important being: hydraulic pumps, hydraulic cylinders, valves, as well as oil filter elements. Linear hydraulic motors are commonly known under the technical name of hydraulic cylinders and are hydraulic elements that define a linear movement with a certain force to the execution mechanism, resulting in the reverse energy conversion of hydrostatic energy to mechanical energy. Thus, the hydraulic energy is converted into an easily controllable force, which acts in a straight line. Spider cranes have hydraulic cylinders with double actuation, bilateral rods, and telescopic cylinders.

Thus, Feng et al. [12] demonstrated that in a mechanical system of a "Spider Crane" driven by hydraulic cylinders, the dynamic response characteristics of the mechanical system are significantly affected by the stiffness characteristics of the hydraulic cylinders by studying the impact of factors such as hydraulic fluid volume, deformation axial movement of the piston rod, expansion of the cylinder volume or deformation of the hydraulic cylinder seal. The influence of the hydraulic pump fluid discharge pressure and the lifting angle of the hook loads was also presented by L. Wu et al. [13] in the case of the synchronization of two hydraulic motors in a lifting system for large cranes.

The paper aims to highlight some concrete aspects regarding the construction and operation of a volumetric pump with variable flow pistons from the construction of a "Spider Crane" type lifting system and the calculation of its functional parameters, aspects regarding the hydraulic parameters that define an actuation cylinder of the system lift and general CAD and FEM models for an actuating cylinder, respectively the load hook, as a mechanism used for lifting weights.

2. CALCULATION OF THE HYDRAULIC PUMPS AND CYLINDERS PARAMETERS

2.1. Parameters of the hydraulic pumps

Pumps are considered primary elements in the structure of hydraulic lifting systems of "Spider Crane" type, which have the role of transforming mechanical energy into hydraulic energy and are designed to generate a power flow

necessary to overcome the pressures developed in the opposite direction of their own load. As a rule, axial pixton-type hydraulic pumps with their ability to adapt to varying flow requirements, due to their low moment of inertia and axial balancing, can operate at high speeds - 1500÷2700 rot./min., and in special cases, at 4000÷20000 rot./min. They circulate flows (*Q*) ranging from 3to 800 l/min at high and very high pressures, p=200÷700 bar [14].

The theoretical flow rate of axial piston pumps is given by the relation:

$$Q = V \cdot n \left[\mathrm{m^3/s} \right],$$ (1)

where *V* is the oil volume discharged at one rotation, in *m³*, *n* is the pump revolution, in *rot/min*.

The oil volume discharged at one rotation of the block is:

$$V = \frac{\pi \cdot d^2}{4} \cdot h \cdot z \left[\mathrm{mm^3} \right],$$ (2)

where *d* is the effective diameter of a piston, in *mm*, *z* - the number of pistons; *h* - the stroke of the piston, in *mm*.

For *n* revolution, the flow rate of the pump with axial pistons is given by the expression:

$$Q = 10^{-6} \cdot \frac{\pi \cdot d^2}{4} \cdot h \cdot z \cdot n \left[\mathrm{l/min} \right].$$ (3)

The stroke of the *h* piston can be calculated with the relation:
- for the pump with inclined block,

$$h = 2 \cdot R \cdot \sin\alpha;$$ (4)

- for the pump with inclined disc,

$$h = 2 \cdot R \cdot tg\alpha;$$ (5)

where *R* is the approximate radius, in *mm*; *α* - inclination angle, defined as an adjustment parameter.

The theoretical flow will be calculated with the relation:
- for the pump with inclined block,

$$Q = \frac{1}{2} \cdot 10^{-6} \cdot \pi \cdot d^2 \cdot R \cdot z \cdot n \cdot \sin\alpha \left[\mathrm{l/min} \right];$$ (6)

- for the pump with inclined disc,

$$Q = \frac{1}{2} \cdot 10^{-6} \cdot \pi \cdot d^2 \cdot R \cdot z \cdot n \cdot tg\alpha \left[\mathrm{l/min} \right].$$ (7)

The moment at the pump is calculated using the *p* pressure and *V* volume, according with the relation:

$$M = \frac{p \cdot V}{2 \cdot \pi} \left[\mathrm{N \cdot m} \right].$$ (8)

At the same time, the power of the electric motor drives the hydraulic pump to the required parameters with the help of pressure, flow and yield:

$$P = \frac{p \cdot Q}{612 \cdot \eta} \left[\text{kW} \right], \tag{9}$$

where η yield is between $0.5 \div 0.9$.

2.2. The calculation development of the hydraulic pumps parameters

In order to determine the parameters of the hydraulic pumps that actuate a crane, a calculation of the flow rate (Q), the moment (M) and the power (P) was performed for several types of pumps, taking into account the volume variables (V) and rotation (n). For the flow calculation, normalized values will be adopted for [14]: revolution: $n=(2000, 2100, 2350, 2500, 2700)$ *rot/min*; volume: $V=(55, 105, 165.5, 250, 331.2)$ *cmc*.

In Tables 1÷5, the flow was calculated for a number of pumps as a function of volume and revolution.

Table 1. Calculation of the flow at a certain variation of the *n* revolution and volume of 55 cmc.

Crt. no.	V1 [cmc]	n [rot/min]	Q [l/min]
1	55	2000	110
2	55	2100	115.5
3	55	2350	129.25
4	55	2500	137.5
5	55	2700	148.5

Table 2. Calculation of the flow at a certain variation of the *n* revolution and volume of 105 cmc.

Crt. no.	V2 [cmc]	n [rot/min]	Q [l/min]
1	105	2000	210
2	105	2100	220.5
3	105	2350	246.75
4	105	2500	262.5
5	105	2700	283.5

Table 3. Calculation of the flow at a certain variation of the *n* revolution and volume of 165.5 cmc.

Crt. no.	V3 [cmc]	n [rot/min]	Q [l/min]
1	165.5	2000	331
2	165.5	2100	347.55
3	165.5	2350	388.925
4	165.5	2500	413.75
5	165.5	2700	446.85

Table 4. Calculation of the flow at a certain variation of the *n* revolution and volume of 250 cmc.

Crt. no.	V4 [cmc]	n [rot/min]	Q [l/min]
1	250	2000	500
2	250	2100	525
3	250	2350	587.5
4	250	2500	625
5	250	2700	675

Table 5. Calculation of the flow at a certain variation of the *n* revolution and volume of 331.2 cmc.

Crt. no.	V5 [cmc]	n [rot/min]	Q [l/min]
1	331.2	2000	662.4
2	331.2	2100	695.52
3	331.2	2350	778.32
4	331.2	2500	828
5	331.2	2700	894.24

In Figure 2, a natural increase in pump flow is observed, an increase due to the change in pump volume. For the calculation of the moment, normalized values will be adopted for:
- pressure: $p=(380, 400, 420, 440, 460)$ *bar*;
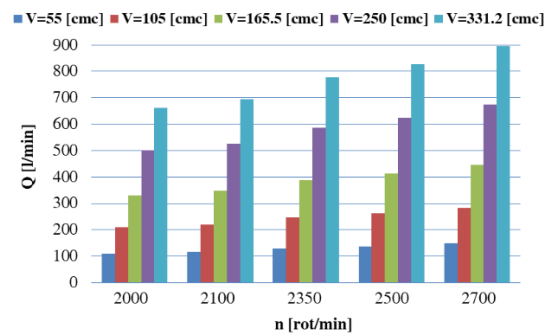- volume: $V=(55, 105, 165.5, 250, 331.2)$ *cmc*.

Fig. 2. Flow rate variation.

In Tables 6÷10 the moment was defined according to pressure and volume.

Table 6. Calculation of the moment at a certain variation of the *p* pressure and volume of 55 cmc.

Crt. no.	V1 [cmc]	p [bar]	M [N·m]
1	55	380	332.63
2	55	400	350.14
3	55	420	367.65
4	55	440	385.16
5	55	460	402.66

Table 7. Calculation of the moment at a certain variation of the *p* pressure and volume of 105 cmc.

Crt. no.	V2 [cmc]	p [bar]	M [N·m]
1	105	380	635.03
2	105	400	668.45
3	105	420	701.87
4	105	440	735.30
5	105	460	768.72

Table 8. Calculation of the moment at a certain variation of the *p* pressure and volume of 165.5 cmc.

Crt. no.	V3 [cmc]	p [bar]	M [N·m]
1	165.5	380	1001.53
2	165.5	400	1054.24
3	165.5	420	1106.95
4	165.5	440	1159.67
5	165.5	460	1212.38

Table 9. Calculation of the moment at a certain variation of the *p* pressure and volume of 250 cmc.

Crt. no.	V4 [cmc]	p [bar]	M [N·m]
1	250	380	1699.46
2	250	400	1788.9
3	250	420	1878.35
4	250	440	1967.79
5	250	460	2057.24

Table 10. Calculation of the moment at a certain variation of the *p* pressure and volume of 331.2 cmc.

Crt. no.	V5 [cmc]	p [bar]	M [N·m]
1	331.2	380	2003.06
2	331.2	400	2108.48
3	331.2	420	2213.91
4	331.2	440	2319.33
5	331.2	460	2424.76

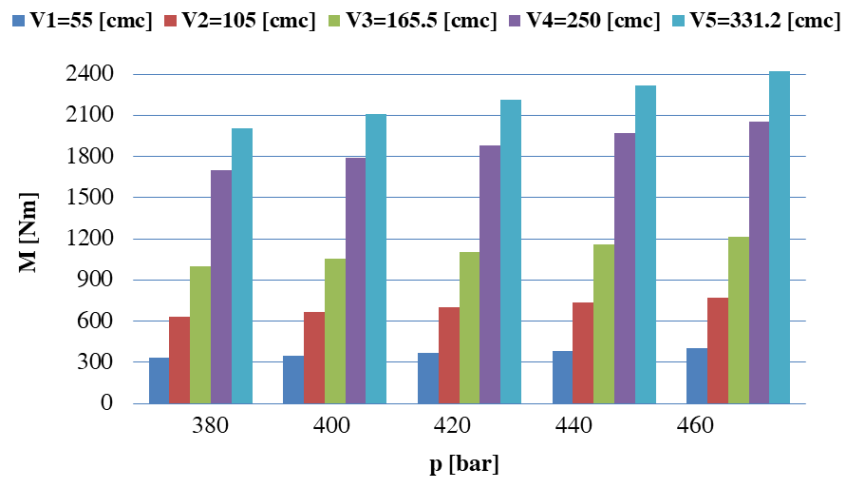The graphical representation of these values is shown in Figure 3.

Fig. 3. Moment variation.

For the calculation of the power, normalized values will be adopted for:
- pressure: p=(380, 400, 420, 440, 460) bar;
- flow: Q=(148.5, 283.5, 446.85, 675, 894.24) l/min.

In Tables 11÷15 the power was defined according to pressure, flow and yield.

Table 11. Calculation of the power at a certain variation of the *p* pressure and flow of 148.5 cmc.

p [bar]	Q1 [l/min]	η	P [kW]
380	148.5	0.9	102.45
400	148.5	0.9	107.84
420	148.5	0.9	113.24
440	148.5	0.9	118.63
460	148.5	0.9	124.02

Table 12. Calculation of the power at a certain variation of the *p* pressure and flow of 283.5 cmc.

p [bar]	Q2 [l/min]	η	P [kW]
380	283.5	0.9	195.59
400	283.5	0.9	205.88
420	283.5	0.9	216.18
440	283.5	0.9	226.47
460	283.5	0.9	236.76

Table 13. Calculation of the power at a certain variation of the *p* pressure and flow of 446.85 cmc.

p [bar]	Q3 [l/min]	η	P [kW]
380	446.85	0.9	308.28
400	446.85	0.9	324.51
420	446.85	0.9	340.74
440	446.85	0.9	356.96
460	446.85	0.9	373.19

Table 14. Calculation of the power at a certain variation of the *p* pressure and flow of 675 cmc.

p [bar]	Q4 [l/min]	η	P [kW]
380	675	0.9	465.69
400	675	0.9	490.20
420	675	0.9	514.71
440	675	0.9	539.22
460	675	0.9	563.73

Table 15. Calculation of the power at a certain variation of the *p* pressure and flow of 894.24 cmc.

p [bar]	Q5 [l/min]	η	P [kW]
380	894.24	0.9	616.94
400	894.24	0.9	649.41
420	894.24	0.9	681.88
440	894.24	0.9	714.35
460	894.24	0.9	746.82

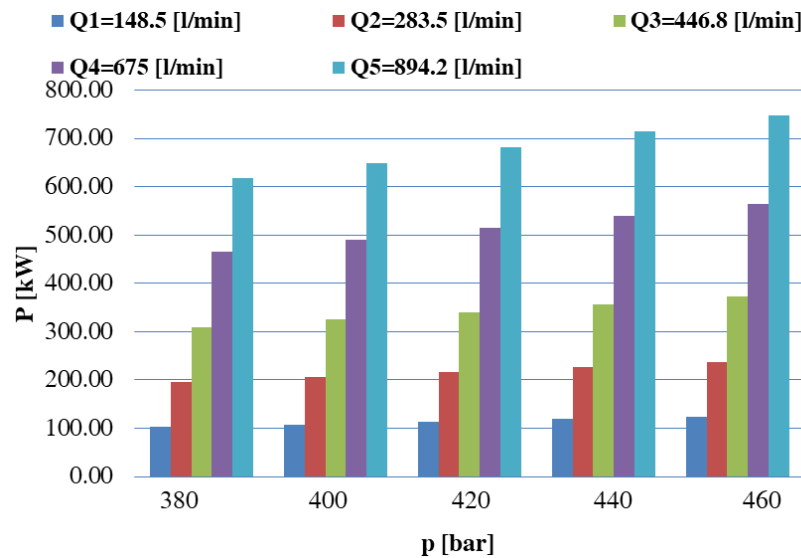The graphical representation of these values is shown in Figure 4.

Fig. 4. Power variation.

2.3. Parameters of the hydraulic cylinders
The average displacement speed v of the piston is determined by the relation:

$$v = \frac{Q_M}{S_p} \ [\text{m/min}],\qquad\qquad(10)$$

where S_p is the effective surface of the piston, Q_M - the value of the oil flow entering the hydraulic cylinder.

The axial force on the piston F_p is calculated with the relation:

$$F_p = p \cdot S_p \ [\text{daN}].\qquad\qquad(11)$$

The required liquid flow rate in the cylinder is calculated with the relation:

$$Q = \frac{S_p \cdot v}{\eta_v} \ [\text{l/min.}],\qquad\qquad(12)$$

where η_v is the volumetric yield.

2.4. The calculation development of the hydraulic cylinders' parameters
Table 16 provides an experimental estimate of hydraulic cylinder speed and force based on flow rate Q, pressure p, diameters D (piston), d (rod) and piston stroke length L.

Table 16. Calculation of the hydraulic cylinders.

Crt. no.	D [mm]	d [mm]	S_1 [mm²]	S_2 [mm²]	Q [l/min]	p [bar]
1	110	63	9503.32	6386.07	50	210
2	110	63	9503.32	6386.07	80	360
3	110	63	9503.32	6386.07	100	400
4	110	63	9503.32	6386.07	120	440
5	110	63	9503.32	6386.07	148.5	460

Crt. no.	L [mm]	v_1 [m/min]	v_2 [m/min]	F_1 [daN]	F_2 [daN]	F_{max} [daN]
1	900	5.26	7.83	19956.97	13410.75	19956.97
2	900	8.42	12.53	34211.94	22989.86	34211.94
3	900	10.52	15.66	38013.27	25544.29	38013.27
4	900	12.63	18.79	41814.60	28098.72	41814.60
5	900	15.63	23.25	43715.26	29375.93	43715.26

Figures 5 and 6 show the variation of the speed according to the flow rate and the variation of the force according to the pressure.
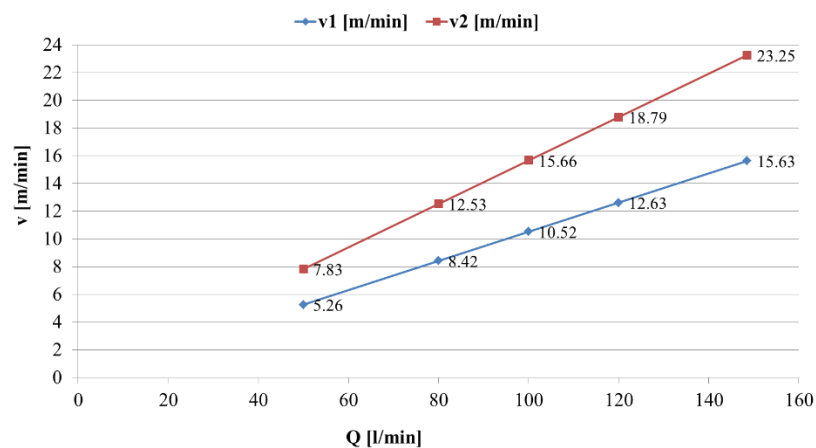
Fig. 5. Variation of the speed.
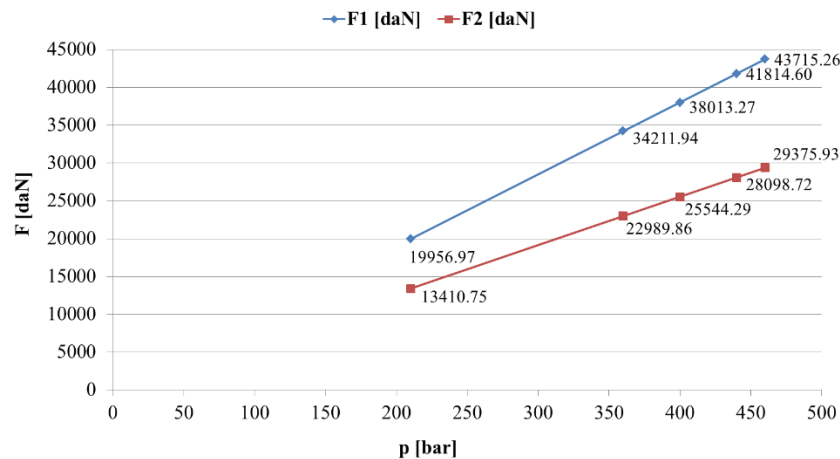
Fig. 6. Variation of the force.

3. DESIGN AND FINITE ELEMENT CALCULATION OF THE LIFTING HOOK AND THE HYDRAULIC CYLINDER

3.1. Design of the lifting hook and the actuator cylinder

Figures 7÷9 show the hydraulic diagrams of the crane's arm: crane arm rest position, Figure 7, when the crane is not in use, or is stationary, its arm being in a balanced position. Under these conditions, the pumping system does not send fluid under pressure into the hydrostatic circuit of the crane; crane arm retracts position, Figure 8, when there is a shortening of the crane arm or a controlled withdrawal of it, which allows greater maneuverability without compromising the crane's lifting capacity; crane arm extension position, Figure 9, when the crane arm is extended or deployed, without exceeding the crane's specified capacity or compromising its stability, with the aim of

reaching long distances. The notations are used: a - hydraulic cylinder; b - pressure regulating valve; c - electric motor; d - hydraulic gear pump; e - manually and electrically controlled 4/3 distributor; f - manometer; g - hydraulic fluid reservoir; h_1 - return line filter; h_2 - pressure line filter; h_3 - pump suction filter.

At the same time, a graphical representation of the hook clamping system from a Spider Crane was made, with the help of the Solid Works program [15], a software package that makes the 3D modeling of solids as concrete and precise as possible. Solid Works has in its composition an integrated series of commands for three-dimensional modeling and the creation of execution and assembly drawings. Thus, both 2D drawing and editing commands, such as Line, Circle, Rectangle, Chamfer, Fillet and 3D modeling commands, such as Extruded Base, Revolved Base, Hole Wizard, Thread etc., were used to model the hook clamping system, each command having its own specific properties.
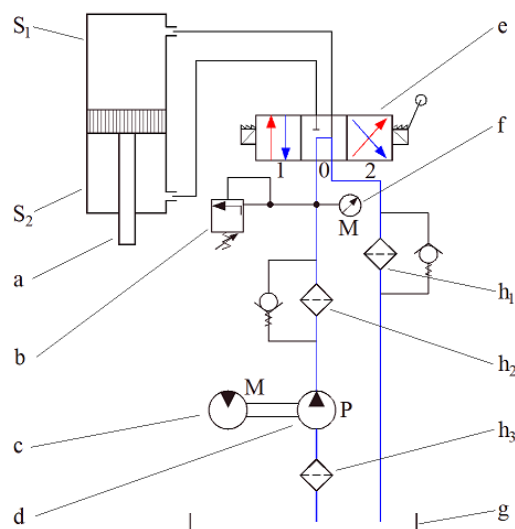
Fig. 7. Crane arm rest position.
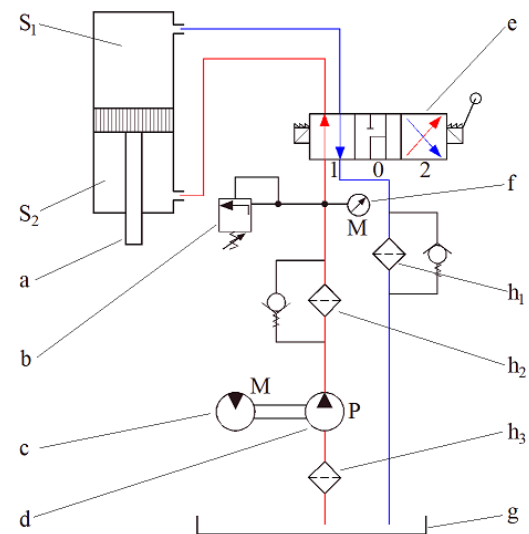
Fig. 8. Crane arm retract position.
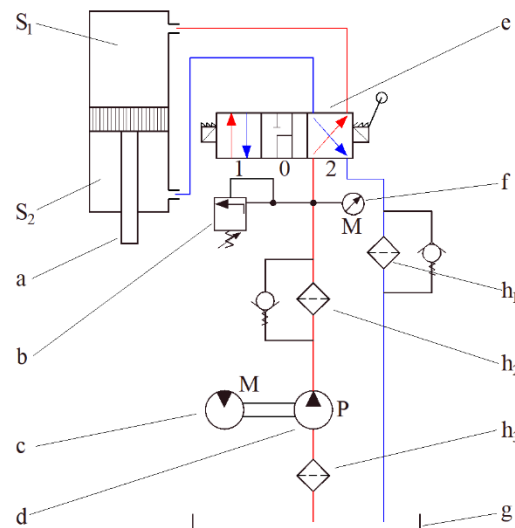
Fig. 9. Crane arm extension position.

Therefore, each component of the hook clamping system is modeled one by one, using the previously mentioned commands, followed by their assembly and obtaining the complete numerical model: the hook, the clamping system of the hook to the stiffening plates, the support plate of the rollers of cable and hook, the threaded shaft for the pulley with the role of stiffening the assembly, the grooved pulley for the cable, the safety pin for the hook, the eyelets for moving the weights and the two nuts: the splined nut for the pin and the self-locking nut for the shafts.

In order to assemble the hook clamping system, constraints are used that help to join all the components of a subassembly or assembly, these being the surface constraints, distance constraints, constraints for establishing the angles between two surfaces, constraints for fixing the main element with the rest of the components etc. Thus, assembling the hook with the clamping nut, then install the spline nut, the two stiffener plates, then install the two threaded shafts for the pulleys, then assemble the grooved pulleys, Figures 10÷14. Finally, after assembling the cables and self-locking nuts for the shafts, the complete virtual model of the hook clamping system of a Spider Crane is obtained, Figure 15.
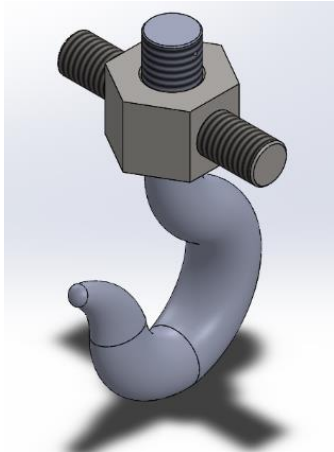
Fig. 10. Assembling the hook with the clamping nut.
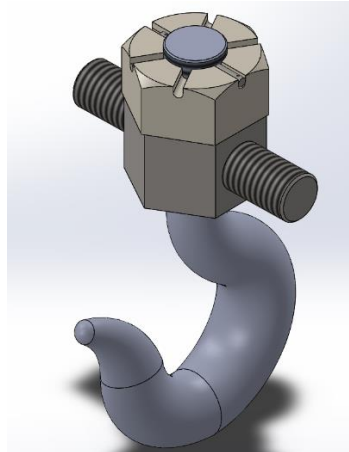
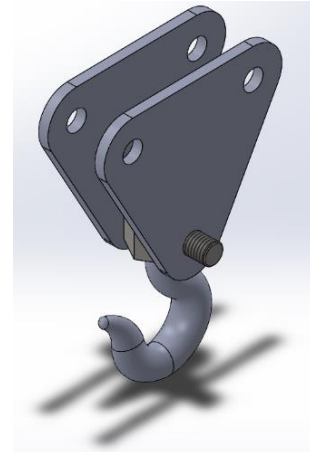Fig. 11. The spline nut installation.

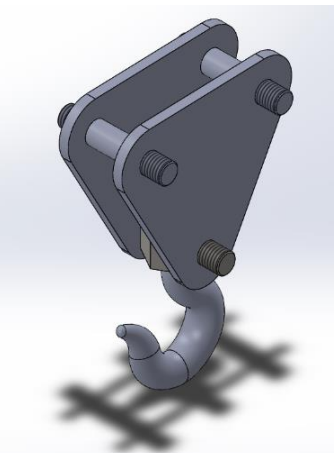Fig. 12. The two stiffener plates assembly.

Fig. 13. Assembling the two threaded shafts for the pulleys.
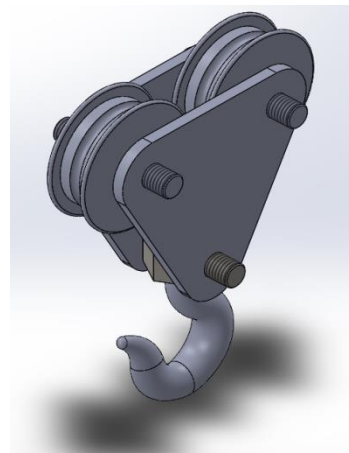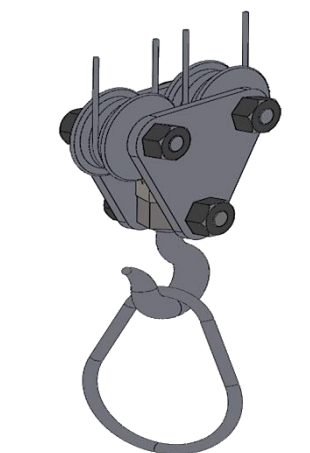

Fig. 14. Assembling the grooved pulleys.

Fig. 15. The virtual model of the hook clamping system.

The graphical modeling of the hydraulic cylinder was also done in the Solid Works program.

3.2. The finite element calculation of the lifting hook and the hydraulic cylinder

Finite element calculation has become a particularly important method in numerically solving a wide range of engineering problems. Each finite element has its own geometric and material characteristics and the calculation takes into account the properties of the materials used, the connection relationships between the elements, the imposed constraints and the loads to which the element is subjected. The finite element analysis of the hook clamping system was carried out using the Ansys program, known in the engineering industry as one of the most advanced and powerful numerical simulation and analysis software [16].

Finite element analysis allowed accurate data on the behavior of the hook clamping system in various situations (Table 17), including under different loads and environmental conditions. This was particularly useful in the hook design and development process, helping to identify potential issues and optimize the design to meet specific performance and safety requirements.

A loading force of 45000 [N] is allowed, applied in the central area of the hook curvature, which is considered to be recessed at the top, the material used in the production of the hook being steel. The equivalent stress and the total deformation of the hook clamping system are shown in Figures 16 and 17.
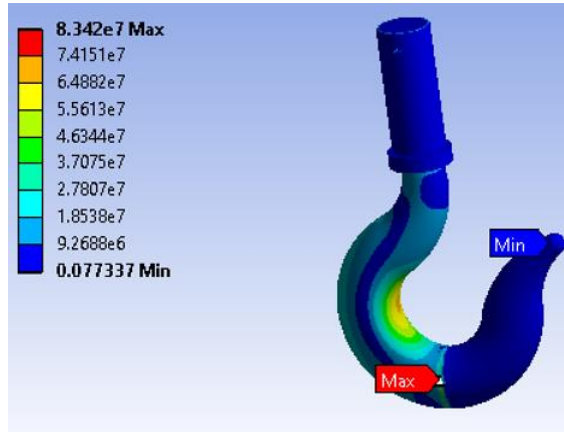

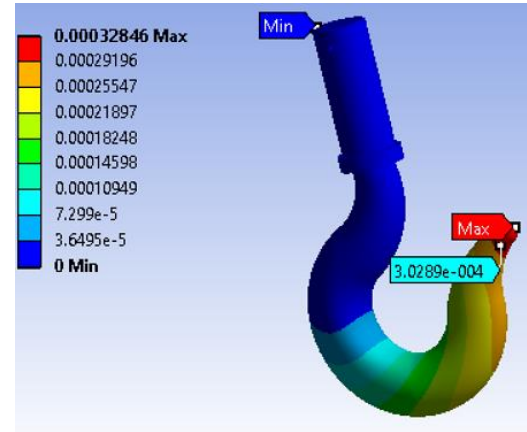Fig. 16. The equivalent stress of the hook clamping system.

Fig. 17. The total deformation of the hook clamping system.

Table 17. Analysis results of the hook clamping system.

	Total deformation [mm]	Equivalent stress [Pa]
Min.	0	0.0773
Max.	0.328	$8.342 \cdot 10^7$

Safety coefficients are also taken into account for these types of hooks to prevent possible accidents. The safety factor taken in this case is 5:1. Thus, the hook is designed to lift a minimum of 4.5 tons, but the safety factor allows it to lift approximately 22 tons.

At the same time, the finite element analysis of the hydraulic cylinder was also realized in Ansys program, their graphical representation being presented in Figures 18 and 19, and the numerical results in Table 18. The hydraulic cylinder was recessed at the bottom and under the action of a force of 50000 [N].
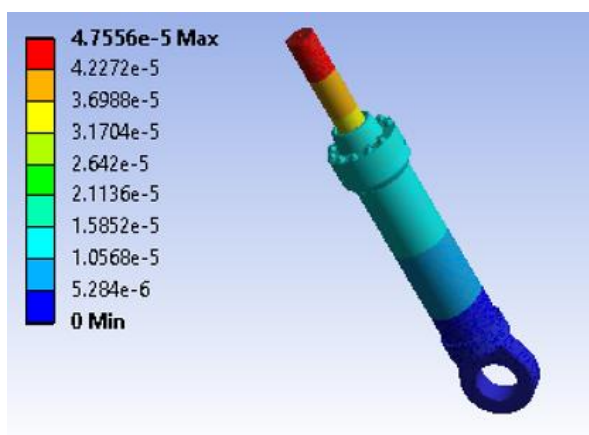

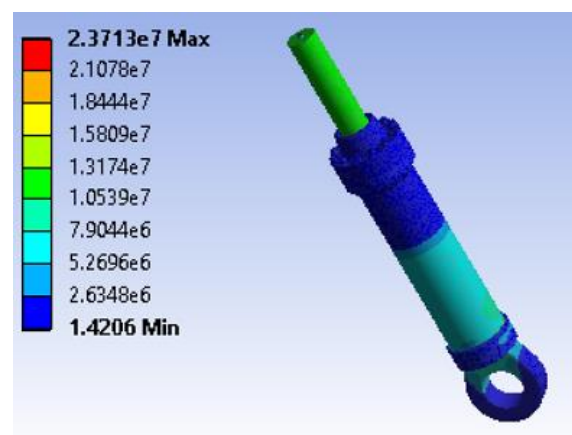Fig. 18. The equivalent stress of the actuator cylinder.

Fig. 19. The total deformation of the actuator cylinder.

Table 18. FEM analysis results of the hydraulic cylinder.

	Total deformation [mm]	Equivalent stress [Pa]
Min.	0	1.4206
Max.	$4.755 \cdot 10^{-5}$	$2.371 \cdot 10^7$

4. CONCLUSIONS

Spider Cranes have multiple advantages, such as better flexibility, compact structure, stable performance and reliability, and are widely used, especially in narrow spaces where standard cranes cannot enter. The stability and reliability of spider cranes are essential factors that enhance their operational efficiency. These cranes are designed to deliver consistent and reliable performance, crucial for tasks that require precision and control. The stability factor is particularly crucial in ensuring safe lifting operations.

The dynamic nature of cranes' hydraulics is a key aspect of their functionality. The correlation between the revolutions of the electric motor, the flow rate of the hydraulic pump and the resulting speed of movement and the force of the hydraulic cylinders illustrate the complexity of their hydraulic systems. This design allows for precise control and adaptability in different operational scenarios. The flow rate of a hydraulic pump varies depending on the number of rotations the electric motor provides to the pump. The movement speed of a hydraulic cylinder varies depending on the surface and flow, and the force depending on the pressure and surface. The design and the calculation with finite elements is necessary in order to observe the behavior of the analyzed parts, thus being able to determine where the parts need to be modified before they are machined, assembled and put to use ensuring that the operator and other workers are not endangered.

It can be stated that Spider-Cranes are built with great ingenuity, they are designed to ease the operator's work and at the same time, they are designed with a very high safety factor, which leads to the protection of the operator; they fold for any kind of activity and are a much cheaper and effective solution than ordinary cranes, of course, for jobs where the lifting demands do not exceed 10-14 tons and heights greater than 40 m.

Data Availability Statement: All data used and analysed in this research are of the authors and are shown in the article.

Conflicts of Interest: The authors declare no conflicts of interest.

REFERENCES

[1] Maeda Mini Cranes, Mini Crawler Cranes, https://www.maeda-minicranes.com/ (03.09.2023).
[2] GGR Group - Furukawa Unic Corporation, Mini Spider Cranes, https://www.ggrgroup.com/products/mini-cranes/ (03.09.2023).
[3] Palazzani Industrie S.P.A., Mini Crawler Cranes, https://www.palazzani-usa.com/ (03.09.2023).
[4] Sevdim, T., Çalik, O.K., Baştürk, S., Static strength and harmonic vibration analysis of the spider crane by computational mechanics software, AURUM Journal of Engineering Systems and Architecture, vol. 3, no. 1, 2019, pp. 35-50.
[5] Li, B., He, X., Liao, J., Wei, Y., Luo, X., Li, S., Wang, Y., Finite element analysis of the chassis in telescopic crawler crane, IOP Conference Series: Journal of Physics, vol. 1939, 2021, pp. 1-6.
[6] Shaikh, A.A., Dineesh, K.D., Lifting capacity enhancement of a crawler crane by improving stability, Journal of Theoretical and Applied Mechanics, vol. 54, no. 1, 2016, pp. 219-227.
[7] Rishmawi, S., Tip-over stability analysis of crawler cranes in heavy lifting applications, Thesis in Master of Science in Mechanical Engineering, The George W. Woodru School of Mechanical Engineering, Georgia Institute of Technology, USA, 2016.
[8] Baroiu, N., Teodor, V.G., Costin, G.A., Constructive-functional analysis of single-rod double-acting hydraulic cylinders, TEHNOMUS Journal - New Technologies and Products in Machine Manufacturing Technologies, vol. 24, 2017, pp. 126-131.
[9] Baroiu, N., Moroșanu, G.A., Graphical modelling and studies on hydraulic pump parameters, Journal of Industrial Design and Engineering Graphics - JIDEG, vol. 15, no. 2, 2020, pp. 7-12.
[10] Huang, L., Dutta, S., Cai, Y., Intelligent virtualization of crane lifting using laser scanning technology, Virtual Reality and Intelligent Hardware, vol. 2, no. 2, 2020, pp. 87-103.

[11] Kamath, A.K., Kazi, F., Singh, N.M., Dynamics and control of 2D Spider Crane: a RHC approach, Proceedings of the 19th International Symposium on Mathematical Theory of Networks and Systems - MTNS, Budapest, Hungary, 2010.

[12] Feng, H., Du, Q., Huang, Y., Chi, Y., Modelling study on stiffness characteristics of hydraulic cylinder under multi-factors, Strojniški vestnik - Journal of Mechanical Engineering, vol. 63, no. 7-8, 2017, pp. 447-456.

[13] Wu, L., Wang, L., Zhang, C., Shi, H., Dynamic characteristics analysis and dual motor synchronous control of hydraulic lifting system for large cranes, The Journal of Engineering, vol. 2019, no. 13, 2019, pp. 203-207.

[14] Linde Hydraulics, Pumps, https://www.linde-hydraulics.com/ (06.09.2023).

[15] SolidWorks 3D CAD, https://cadworks.ro/ (21.03.2023).

[16] Ansys Workbench, https://www.ansys.com/products/ansys-workbench (14.04.2023).